Available online at www.sciencedirect.com
ScienceDirect
Acta Materialia 57 (2009) 1660–1665
Acta MATERIALIA
www.elsevier.com/locate/actamat

Stability and instability of long-period superstructures in binary Cu–Pd alloys: A first principles study

Stefan Bärthlein [a], Elke Winning [a], Gus L.W. Hart [b], Stefan Müller [a,*]

[a] University Erlangen-Nürnberg, Lehrstuhl für Festkörperphysik, Staudtstr. 7 D-91058 Erlangen, Germany
[b] Department of Physics and Astronomy, Brigham Young University, Provo, UT 84602, USA

Received 7 October 2008; received in revised form 2 December 2008; accepted 7 December 2008
Available online 24 January 2009

Abstract

Whereas binary intermetallic compounds often appear as ordered structures with fewer than 10 atoms per cell, large-supercell structures consisting of one- and two-dimensional superstructures have long been observed in CuPd. However, whereas the stability of the ordinary one-dimensional long-period superstructures (1-D LPS) has been previously investigated by first-principles total-energy methods, two-dimensional superstructures were not amenable to such calculations because of their large number of atoms ($\mathcal{O}(10^3)$ atoms/cell). Using a cluster expansion extracted from a set of first-principles total energy calculations, we show that 2-D LPSs are likely kinetically-stabilized structures which transform into the 1-D LPS ground-state structures at thermodynamic equilibrium.

Keywords: Copper alloys; Intermetallic compounds; Density functional theory; Cluster expansion; MC-simulation

1. Introduction

Our understanding of the basic rules governing the phase-stability of intermetallic compounds rests, to a large extent, on the observation of rather simple, few-atom/cell crystal structures [1,2] such as $L1_0$, $L1_1$, $L1_2$, $D0_{22}$, B2 and B32, which appear repeatedly in the compendia of alloy phase diagrams [3]. However, even in binary systems, the emergence of surprisingly complex structures with thousands of atoms per cell can be implied, as predicted for the CuAu and NiPt systems [4]. In the case of FeCo, a quasicontinuous sequence of ground states was found [5] that consisted of large cell structures differing from each other by just a few atoms.

A second case of complex phases in binary systems are one- or two-dimensional superstructures [6–19], where a sequence of $L1_2$ units (Fig. 1) is repeated in one or two dimensions with periodic antiphase boundaries. However, it is not clear whether these structures represent thermodynamically stable ground states (in which case, one needs to include such structures in developing our understanding of structure and bonding [20]), or if such structures are kinetically stabilized "excited states".

For one-dimensional long-period superstructures (1-D LPSs) in CuPd, effective interactions have been obtained (i) via the axial next-nearest neighbor Ising model (ANNNI) [21], based on local density approximation (LDA) calculations; (ii) with the generalized perturbation method (GPM), by expanding the electronic energy about the disordered state using the coherent potential approximation (CPA) [22]; and (iii) using the mixed-space cluster expansion approach [23]. Also, one study that coupled CPA with the Bragg–Williams mean-field approach agreed well with experiments in Ref. [24], but was restricted to 1-D LPSs.

For 1-D CuPd structures there is a broad agreement [10] that these structures are thermodynamic stable states, but for 2-D LPS the situation is more complex due to controversal experimental results (see, e.g., [6,10]). There has been no first-principles study of the energetics of these 2-D-structures because this requires large ($\mathcal{O}(10^3)$ atoms) unit

* Corresponding author. Tel.: +49 9131 85 28408; fax: +49 9131 85 28400.
E-mail address: stefan.mueller@physik.uni-erlangen.de (S. Müller).

1359-6454/$34.00 © 2008 Acta Materialia Inc. Published by Elsevier Ltd. All rights reserved.
doi:10.1016/j.actamat.2008.12.013

cells. We have recently developed [25] an accurate cluster expansion for CuPd, finding new small-cell ground state structures explaining the previously assumed $L1_2$ structure (see S1, S2, and S3 in Fig. 3). We now address the stability of 1- and 2-D LPSs in CuPd and find that 1-D LPSs are ground states but 2-D LPSs are not.

2. Structure of 1- and 2-D LPS

Fig. 1 shows how 1-D LPSs at A_3B stoichiometry (from which the 2-D LPSs should evolve according to Ref. [6]) are constructed by stacking $L1_2$ units in the z-direction and introducing regular (periodic) anti-phase shifts. There are three possible anti-phase shifts, as shown in the figure (right). When the anti-phase shift is in the stacking plane, $\mathbf{a}_I = (0,1/2,1/2)$, the resulting antiphase boundary (APB) is referred to as a type I APB. This the only antiphase shift observed in 1-D LPS. One-dimensional LPSs constructed by small-period APB stacking, like $M = 1$ or 2, occur commonly in alloys and are referred to by "Strukturberichte" names like $D0_{22}$ and $D0_{23}$. Higher-period structures are referred to as LPS M, where M is the period, or briefly $\langle M_z \rangle$ [26].

Two-dimensional LPSs have two sets of APBs, one in each stacking direction. In two dimensions, the degeneracy of the second kind of APBs is broken, resulting in two kinds of type II APBs, referred to as IIa and IIb [27]. Although type II APBs have not been observed in 1-D LPSs, they have been observed in 2-D LPSs. Fig. 2 depicts the most interesting 2-D LPS candidates featured in the studies of Terasaki et al. [8,9] and Broddin et al. [6,14,15] at finite temperatures. Following the nomenclature introduced with their first appearance in the literature [7], we refer to a structure with type I APBs in one direction and type IIa APBs in the other (i.e. $M_I = M_{IIa} = 1$) as $\langle 1_x 1_z \rangle$. The energies of 2-D LPSs $\Delta H_f(M_x M_z)$ are expected to asymptotically approach those of 1-D LPSs $\Delta H_f(M_z)$ according to

$$\lim_{M_x \to \infty} \Delta H_f(M_x M_z) = \Delta H_f(M_z) \tag{1}$$

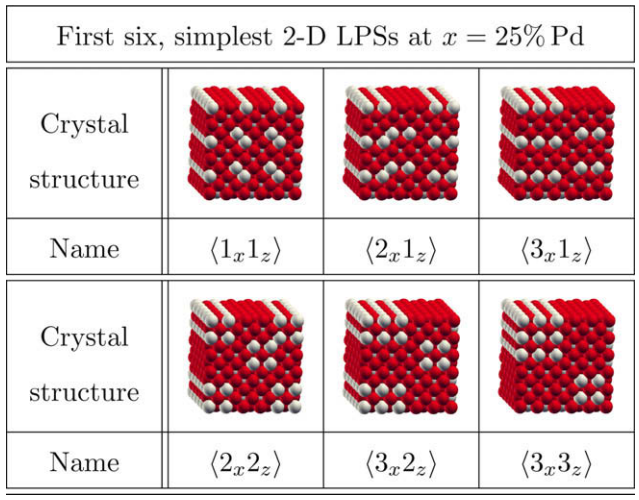

Fig. 2. Six of the smallest 2-D LPSs possible at 25%Pd. All of them belong to type I + IIa.

3. Method

To adequately treat the long-range strain that occurs in stacked 1- and 2-D LPSs, one needs a model that goes beyond short-range, real-space interactions. Though direct calculation of the energetics of 2-D LPSs is desirable, the calculations are impractical due to both the sheer size of

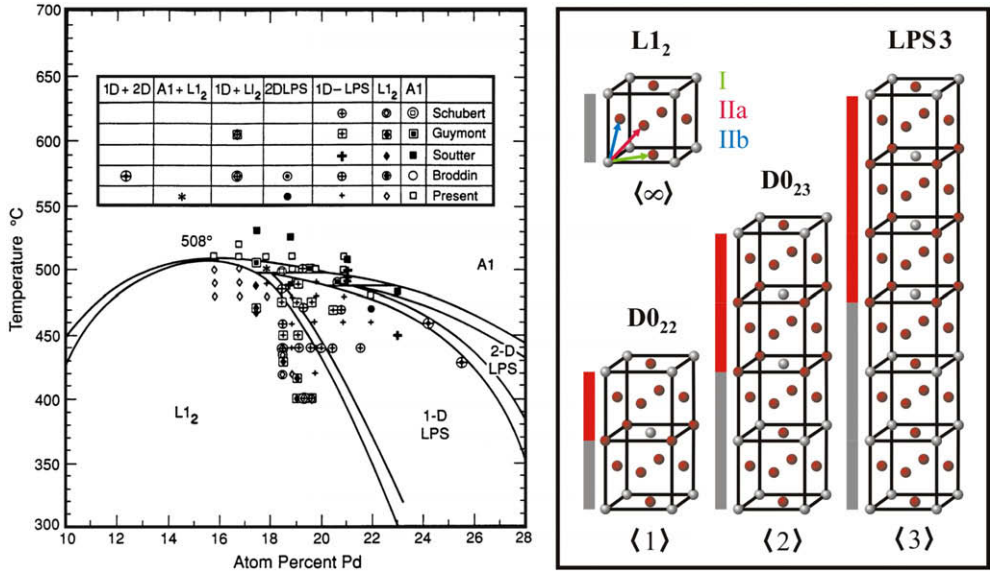

Fig. 1. (Left) The Cu-rich part of the CuPd phase diagram as assessed by experimentation [10]. Whereas 1-D LPSs are stable down to low temperatures, the thermodynamic stability of 2-D LPSs is questionable due to conflicting experimental observations. (Right) Construction of simple 1-D superstructures using $L1_2$ building blocks. Note that for $L1_2$ there are three possible "out-of-step" directions: I = (1/2,1/2,0), IIa = (1/2,0,1/2) and IIb = (0,1/2,1/2).

the unit cell and the number of different APB configurations. The cluster-expansion (CE) method [28] provides an efficient framework for a systematic description of large cell sizes with density functional theory accuracy.

Using the mixed-space CE formalism [29], effective interactions define a simple Hamiltonian that can rapidly predict the energetics of arbitrary configurations with first-principles accuracy and with the correct strain energy in the long-period limit. First, formation enthalpies ΔH_f (per atom) of geometrically fully relaxed structures are obtained from first principles. These energies are mapped onto an Ising-like Hamiltonian:

$$\Delta H_{CE}(\sigma) = \sum_{\mathbf{k}} J_{pair}(\mathbf{k})|S(\mathbf{k},\sigma)|^2 + \sum_{f}^{MBITs} D_f J_f \bar{\Pi}_f(\sigma) + \frac{1}{4x-1}\sum_{\mathbf{k}} J_{CS}(x,\hat{\mathbf{k}})|S(\mathbf{k},\sigma)|^2 \quad (2)$$

This formalism expands the formation enthalpy in a cluster-by-cluster sum over all the sites in the unit cell. For each figure (cluster) f, the lattice-averaged "spin" product $\bar{\Pi}_f(\sigma)$ is computed for the atomic configuration, σ, of the structure being expanded. This so-called correlation function, $\bar{\Pi}_f$, weighted by its geometric degeneracy D_f, is multiplied by the effective energy J_f. A sum over all possible clusters is a mathematically complete expansion for a structure's formation enthalpy [28]. To yield accurate energies for long-period superstructures, we treat pair interactions and strain energy in reciprocal space. The CE Hamiltonian is truncated to a relatively small number of terms using an evolutionary approach [31,30]. Subsequently, the energies of $\mathcal{O}(10^6)$ structures are predicted by a systematic ground-state search (GSS), shown in Fig. 3. The resulting convex hull yields the ground-state line and serves as a basis for an extended GSS, including arbitrary LPSs with up to 10,000 atoms per unit cell.

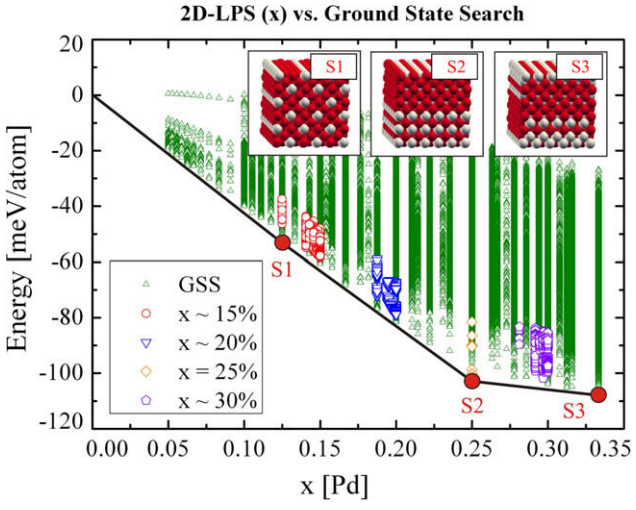

Fig. 3. Stability diagram for $0\% \leqslant x_{Pd} \leqslant 33\%$. The ground state structures S1, S2 and S3 are depicted in the three insets and discussed in more detail in Ref. [25]. Remarkably, the cluster expansion is capable of a consistent description of 2-D LPSs even at off-stoichiometry (polygonal symbols).

Table 1
LDA values versus predicted energies from the cluster expansion. "Equiv." energies are based on an equivalent k-point mesh. For larger cells, the difference method "Diff." is used, which for smaller cells also yields good agreement in hierarchy and absolute values. In $^{(*)}$ all energies are referred to $\Delta H_f(L1_2)$. Ground-state energies are bold-face

$\langle\{M_i\}\rangle$	Equiv.	Diff.$^{(*)}$	CE	Ref. [21]
1-D LPSs				
∞	−98.8	−98.8	−100.9	−99.6
1_z	−89.9	−89.7	−89.9	−91.7
2_z	−100.1	−99.5	−101.2	−98.5
3_z	**−102.8**	**−102.4**	**−102.2**	**−102.5**
4_z	−101.7	−102.2	−101.3	–
5_z	−100.7	−101.2	−101.2	–
6_z	−100.3	−100.5	−101.1	–
2-D LPSs				
1_x1_z	−75.6	−76.2	−77.6	–
2_x1_z	−85.8	−83.8	−84.0	–
3_x1_z	−88.1	−88.6	−86.4	–
2_x2_z	–	−97.4	−96.8	–
3_x2_z	–	−97.8	−96.7	–
3_x3_z	–	−96.3	−96.8	–

Calculating the formation enthalpies for the 2-D LPSs that were included in the construction of the CE required an adapted approach. Based on a $10 \times 10 \times 10$ k-point mesh for the basic cell, the mesh along the y-axis was fixed, whereas the number of k-points was reduced along the other two directions according to the increase in M_x and M_z. For 1-D LPSs, only k_z was adjusted. For all LPSs, the corresponding $L1_2$-blocks were treated in the same k-mesh. As far as possible, the convergence of the energy *differences* $E_M - E_{L1_2}$ was controlled by a direct calculation based on a $19 \times 19 \times 19$ k-point mesh (denoted "Equiv." in Table 1). Table 1 gives the 1- and 2-D LPS energies as obtained from LDA. The first column shows that the 2-D LPSs are converging towards the corresponding 1-D LPS limit.

Our CE is clearly capable of predicting all 2-D LPSs well, within an accuracy of 1-2 meV atom^{-1}. More importantly, the hierarchy of the 2-D LPSs is correctly reproduced. This level of accuracy is required for our GSSs and Monte Carlo simulations.

4. Ground state behavior

The GSS shown in Fig. 3 shows the energies of $\mathcal{O}(10^6)$ structures. These structures are all face-centered cubic-based structures containing 20 atoms or less per unit cell for concentrations in the range $0 \leqslant x \leqslant 33\%$. This list includes 1- and 2-D LPSs for small periods ($\langle M_z\rangle \leqslant \langle 5_z\rangle$, $\langle M_x M_z\rangle = \langle 1_x 1_z\rangle$). The energies for larger 2-D LPSs, indicated by colored symbols, were predicted in a separate step; the results are discussed in the following.

For the six smallest 2-D LPSs with ideal stoichiometry constructable in the I–IIa combination, LDA energies and their predictions by CE are listed in Table 1. From

the trend of the 1-D LPSs, we see that a higher density of APBs is not favorable with respect to the ground state LPS 3, so presumably APBs in 2-D LPSs are even more energetically unfavorable. In fact, all small 2-D LPSs are less stable (higher in energy) than the simple 1-D LPSs with $M \leqslant 2$. On the other hand, there is a clear tendency for 2-D LPSs to turn into 1-D-like LPSs for large M, which is also reflected by their energies: $\lim_{M_x\to\infty}\Delta H_{\langle M_xM_z\rangle} = \Delta H_{\langle M_z\rangle}$.

In addition to the I–IIa-type 2-D LPSs that have been observed, there are other possible types with different APBs, and we need to include these as well in our GSS. Taking all nine binary combinations of the three different APB types, {I,IIa,IIb}, there are six non-equivalent combinations; that is, there are six different kinds of 2-D LPSs. We computed the energies for the 100 smallest 2-D LPSs of each kind, two of which are shown in Fig. 4. Although each 2-D LPS will become a 1-D LPS when one of the periods becomes very large, for small periods only the I–IIa combination results in low-energy structures that might be stable in some region of the phase diagram (Fig. 1).

To effectively rule out the possibility of thermodynamically stable 2-D LPSs, we also examined off-stoichometry structures at several concentrations, $x_{Pd} \approx \{15\%, 20\%, 30\%\}$. For this, we randomly exchanged Cu and Pd atoms in 2-D LPSs-based supercells to probe the energetics of these kinds of 2-D LPSs. The results are plotted with our GSS in Fig. 3: for each concentration, the energies for the 100 smallest 2-D LPSs are predicted *50* times for randomly generated configurations, resulting in 5000 predictions at each concentration. Their energetic position is displayed by polygon symbols. We find that there are no new ground states predicted, although even at off-stoichiometry the sequence of low-energy structures has a high density imposed by their near degeneracy.

5. Finite temperature properties

As mentioned in the Introduction, type I+IIa 2-D LPSs are sometimes observed experimentally in CuPd. Therefore, we used the Monte Carlo method to test their thermodymical stability at finite temperatures. Because the cluster expansion Hamiltonian can be evaluted rapidly, we can model 2-D LPSs using a large 512,000 atom simulation cell. As both Terasaki and Broddin obtained experimental evidence of 2-D LPSs at 28% Pd around 400°, we performed a thermodynamic Monte Carlo simulation in order to find the equilibrium for this specific situation. To verify that the final results were independent of the starting configuration, we used three different kinds of starting configurations: random configurations, 1-D LPS-like configurations and 2-D LPS-like configurations. In all cases, the simulations come into equilibrium with a LPS 3-like configuration containing a few antisites (that are necessary due to the excess Pd atoms). Simulations using starting configurations that were LPS-like were repeated with three different starting configurations: (i) $\langle 4_x3_z\rangle$-like, (ii) $\langle 3_x2_z\rangle$-like and (iii) a 1-D LPS 3. Each had randomly added excess atoms. Although more starting configurations could be tested, the energetic behavior suggested by the predictions in Fig. 5 indicate that, assuming vibrational enthalpy is not significant, 2-D LPSs are not a stable feature of the CuPd phase diagram. One possible solution would be that 2-D LPSs are kinetically stabilized. Such an investigation demands a detailed knowledge of the activation barriers for the relevant diffusion processes as recently performed for Al-rich alloys [32]. Here, we focus on the thermodynamic properties.

Returning to Table 1, it should be noted that the lowest-energy 2-D LPS, $\langle 3_x2_z\rangle$, has a lower symmetry than $\langle 3_x3_z\rangle$. Interestingly, experimentalists also find asymmetric structures such as $\langle 4.26_x3.40_z\rangle$ at $T = 340°$ in $Cu_{0.72}Pd_{0.28}$ [8].

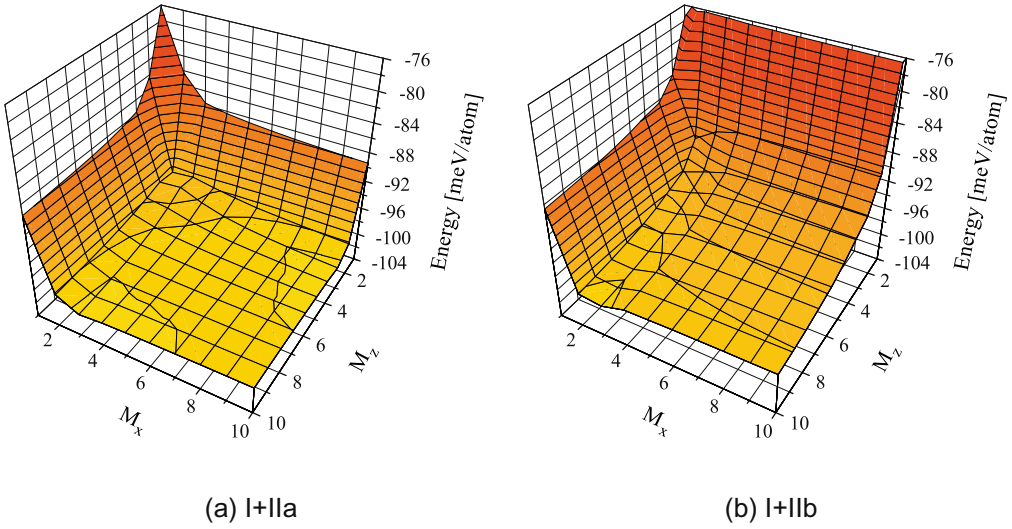

Fig. 4. Energetics for two of the six nonequivalent 2-D LPS motifs as a function of M_z and M_x. The experimentally observed combination I + IIa has an energy close to that of the ground state 1-D LPS 3 for higher periods in x-direction. Other APB combinations, I + I, IIa + I, IIa + IIb and IIb + IIb, are less favorable than I + IIa.

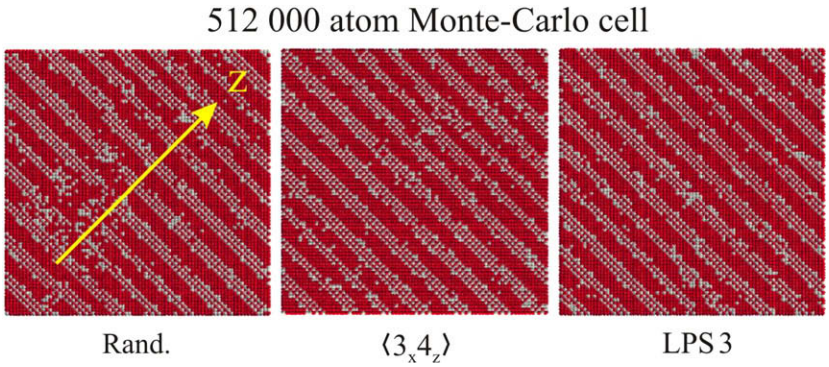

Fig. 5. Equilibrium configuration of simulated annealing Monte Carlo for 512,000 atoms for 28%Pd at 400°, starting from a random configuration (left), $\langle 3_x 4_z \rangle$ (center) and LPS 3 (right). In all cases, the final configuration is 1-D LPS 3-like and not a 2-D LPS.

Moreover, Takeda et al. [33] found a strong concentration dependence of the average modulation wavelength, M_{eff}, i.e. the average length between two antiphase boundaries. Our starting point should be able to confirm these observations and thus confirm the quality of the constructed effective cluster interactions. For this, we perfomed Monte-Carlo simulations for Pd concentrations $0.12 \leqslant x_{Pd} \leqslant 0.30$ using again a 512,000 atom simulation cell. A temperature of $T = 800$ K was chosen, at which no long-range order is observed. The dependence of the bulk conentration on M_{eff} can be studied efficiently by analyzing the diffuse intensities in diffraction patterns caused by substitutional ordering of the system. In order to quantify this intensity, the short-range order (SRO) behavior of the system is described in terms of the Warren–Cowley SRO parameters which are given for shell (lmn) by

$$\alpha_{lmn}(x) = 1 - \frac{P^{A(B)}_{lmn}}{x} \tag{3}$$

where $P^{A(B)}_{lmn}$ is the conditional probability that, given an A atom at the origin, there is a B atom at (lmn). The sign of α indicates qualitatively whether atoms in a given shell prefer to order ($\alpha < 0$) or cluster ($\alpha > 0$). The SRO parameter can be written in terms of the cluster expansion pair correlations as

$$\alpha_{lmn}(x) = \frac{\langle \bar{\Pi}_{lmn} \rangle - q^2}{1 - q^2} \tag{4}$$

where $q = 2x - 1$ and $\langle \bar{\Pi}_{lmn} \rangle$ is the pair correlation function for shell (lmn). In diffraction experiments the portion of diffuse scattering due to SRO is proportional to the lattice Fourier transform of $\alpha_{lmn}(x)$:

$$\alpha(x, \mathbf{k}) = \sum_{lmn}^{n_R} \alpha_{lmn}(x) e^{i \cdot \mathbf{k} \cdot \mathbf{R}_{lmn}} \tag{5}$$

where n_R stands for the number of real space shells used in the transform. Since the LPS group possesses the fundamental reciprocal space wave vector $\mathbf{k} = \langle 1 \frac{1}{2M_{eff}} 0 \rangle$, we have calculated the diffuse intensities for the $X - \Gamma - X$ plane in k-space. The resulting patterns are displayed in Fig. 6 for three selected Pd concentrations: The four SRO peaks around the X-point start to move away from the X-center as concentration increases. In agreement with experimental data, this leads to a clear dependence of M_{eff} on the bulk concentration as shown in Fig. 7.

Our predicted SRO behavior even bears a quantitative comparison with experiment [34]. This is visualized in k-space for a $Cu_{70.2}Pd_{29.8}$ at $T = 773$ K (Fig. 8). A detailed analysis of this diffraction pattern is given in Ref. [25].

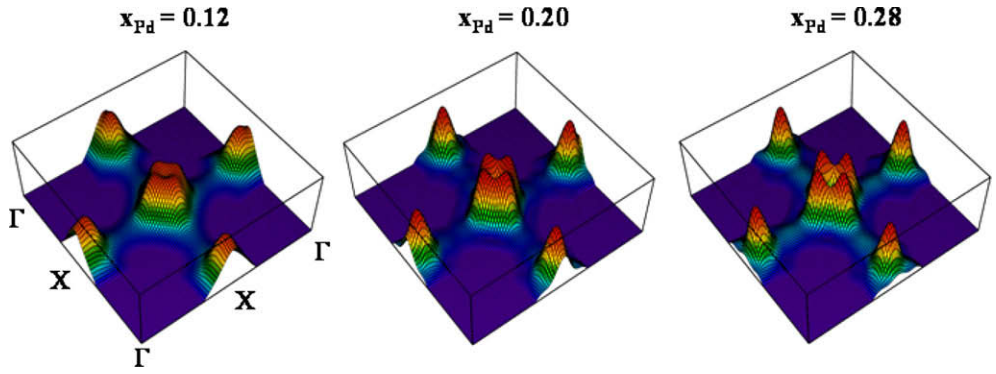

Fig. 6. SRO pattern for $x_{Pd} = 0.12, 0.20, 0.28$ at $T = 800$ K. The increase in the peak splitting around the X-point reflects the change in the average modulation wavelength with increasing Pd concentration.

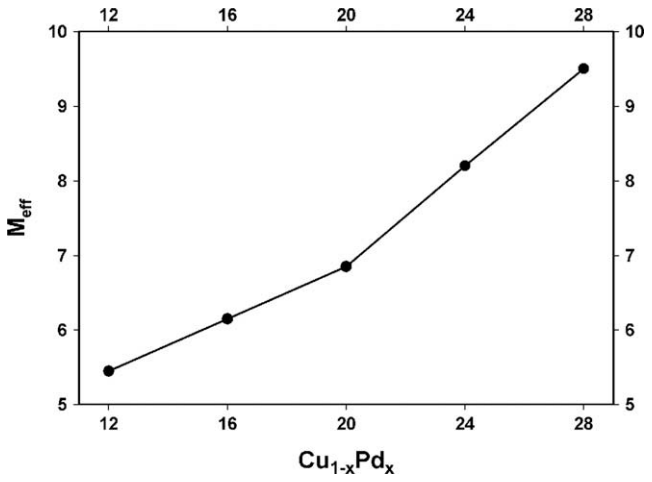

Fig. 7. Dependence of the average modulation wavelength on the bulk concentration (calculated for $T = 800$ K).

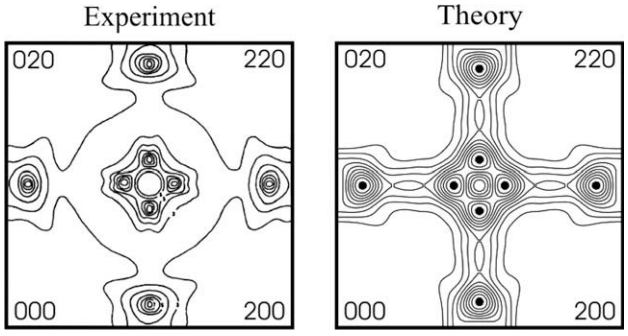

Fig. 8. SRO for $Cu_{70.2}Pd_{29.8}$ at 773 K. Experimental [34] and theoretical data are in excellent agreement (for details, see Ref. [25]).

6. Summary

In summary, we find that 2-D LPSs are not ground-state candidates in CuPd, nor are they stable at finite temperatures in the single-phase region previously assigned to a 2-D LPSs. Instead, decomposition into a 1-D LPSs should occur, but presumably this decomposition is suppressed by kinetic barriers. Finally, we have shown that our approach is able to describe the rather complex SRO behavior of the system, in agreement with earlier experimental investigations.

Acknowledgements

S.B., E.W. and S.M. gratefully acknowledge support by DFG, Mu1648/3 (Germany). G.L.W.H. is grateful to NSF, DMR 0650406 for financial support.

References

[1] Pearson WB. The crystal chemistry and physics of metals and alloys. New York: Wiley; 1972.
[2] Villars P, Calvert LD. Pearson's handbook of crystallographic data. Metals Park, OH: ASM International; 1991.
[3] Massalski TB. In: Murray JL, Bennett LH, Baker H, editors. Binary alloy phase diagrams. Metals Park, OH: American Society for Metals; 1986.
[4] Sanati M, Wang LG, Zunger A. Phys Rev Lett 2003;90:045502.
[5] Drautz R, Diaz-Ortiz A, Fähnle M, Dosch H. Phys Rev Lett 2004;93:067202.
[6] Broddin D, Van Tendeloo G, Van Landuyt J, Amelinckx S. Phil Mag A 1989;59:47.
[7] Watanabe D, Hirabayashi M, Ogawa S. Acta Cryst 1955;8:510.
[8] Terasaki O, Watanabe D. Japan J Appl Phys 1981;20:L381.
[9] Terasaki O. J Phys C: Solid State Phys 1981;14:L933.
[10] Huang P, Menon S, de Fontaine D. J Phase Equilibria 1991;12:3.
[11] Schubert K, Kiefer B, Wilkens M, Haufler R. Z Metallkd 1955;46:692.
[12] Soutter A, Colson A, Hertz J. Mém Sci Rev Metall 1971;68:575.
[13] Guymont M, Gratias D. Phys Status Solidi 1976;36:329.
[14] Broddin D et al. Phil Mag A 1986;54:395.
[15] Broddin D et al. Phil Mag B 1988;57:31.
[16] Hultgren R et al. Selected values of the thermodynamic properties of binary alloys. Metals Park, OH: American Society for Metals; 1973.
[17] Hansen M. Constitution of binary alloys. New York: McGraw-Hill; 1958. p. 612–15.
[18] Predel B. Landolt-Börnstein: numerical data and functional relationships in science and technology – New Series Group 4: Physical Chemistry Group IV, Physical Chemistry. Vol. 5d. Phase Equilibria, crystallographic and thermodynamic data of binary alloys. Berlin: Springer-Verlag;1994, p. 217–22.
[19] Müller S, Zunger A. Phys Rev B 2001;63:094204.
[20] Hume-Rothery W, Smallman RE, Haworth CW. Structure of metals and alloys. London: Institute of Metals; 1969.
[21] Colinet C, Pasturel A. Phil Mag B 2002;82:1067.
[22] Ruban AV, Shallcross S, Simak SI, Skriver HL. Phys Rev B 2004;70:125115.
[23] Lu ZW, Laks DB, Wei SH, Zunger A. Phys Rev B 1994;50:6642.
[24] Ceder G, de Fontaine D, Dreysse H, Nicholson DM, Stocks GM, Gyorffy BL. Acta Metall Mater 1990;38:2299.
[25] Bärthlein S, Hart GLW, Zunger A, Müller S. J Phys: Condensed Matter 2007;19:032201.
[26] Fisher ME, Selke W. Phys Rev Lett 1980;44:1502.
[27] Sato H, Toth RS. Phys Rev 1962;127:469.
[28] Sanchez JM, Ducastelle F, Gratias D. Physica A 1984;128:334.
[29] Laks DB, Ferreira LG, Froyen S, Zunger A. Phys Rev B 1992;46:12587.
[30] Blum V, Hart GLW, Walorski MJ, Zunger A. Phys Rev B 2005;72:165113.
[31] Hart GLW, Blum V, Walorski J, Zunger A. Nat Mat 2005;4:391.
[32] Müller S, Wolf W, Podloucky R. Alloy physics, W. Pfeiler, editor. Weinheim: Wiley-VCH; 2007, p. 589–652.
[33] Takeda S, Kulik J, de Fontaine D. J Phys F 1988;18:1387.
[34] Oshima K, Watanabe D. Acta Cryst A 1976;32:883.